FULL PAPER

Dalton
www.rsc.org/dalton

Redox chemosensors: coordination chemistry towards Cu^{II}, Zn^{II}, Cd^{II}, Hg^{II}, and Pb^{II} of 1-aza-4,10-dithia-7-oxacyclododecane ([12]aneNS$_2$O) and its *N*-ferrocenylmethyl derivative †

Claudia Caltagirone,[a] Andrea Bencini,[b] Francesco Demartin,[c] Francesco A. Devillanova,[a] Alessandra Garau,[a] Francesco Isaia,[a] Vito Lippolis,*[a] Palma Mariani,[b] Ulrich Papke,[d] Lorenzo Tei[a] and Gaetano Verani[a]

[a] *Dipartimento di Chimica Inorganica ed Analitica, Università degli Studi di Cagliari, SS 554 Bivio per Sestu, 09042 Monserrato (CA), Italy*

[b] *Dipartimento di Chimica, Università di Firenze, Via della Lastruccia 3, 50019, Sesto Fiorentino, Florence, Italy*

[c] *Dipartimento di Chimica Strutturale e Stereochimica Inorganica, Università di Milano, Via G. Venezian 21, 20133 Milano, Italy*

[d] *Institut für Organische Chemie der Technischen Universität, Braunschweig, Hagenring 30, D 38106 Braunschweig, Germany*

Received 4th November 2002, Accepted 2nd January 2003
First published as an Advance Article on the web 5th February 2003

The coordination chemistry of the mixed donor 12-membered macrocyclic ligand 1-aza-4,10-dithia-7-oxacyclododecane ([12]aneNS$_2$O) with Cu^{II}, Zn^{II}, Cd^{II}, Hg^{II}, and Pb^{II} has been investigated both in water solution and in the solid state. The protonation constant for [12]aneNS$_2$O and stability constants with the aforementioned metal ions have been determined potentiometrically and compared with those reported for other mixed N/S/O-donor tetradentate 12-membered macrocycles. The measured values are consistent with trends observed previously for aza macrocycles as secondary N-donors are replaced by O- and S-donors. In particular our results show that Hg^{II} in water has the highest affinity for [12]aneNS$_2$O followed by Cu^{II}, Cd^{II}, Pb^{II}, and Zn^{II}. For each considered metal ion, 1 : 1 complexes of [12]aneNS$_2$O have been isolated in the solid state; those of Cu^{II}, Hg^{II}, and Cd^{II} have also been characterised by X-ray crystallography. In the cases of copper(II) and cadmium(II) complexes the ligand adopts a folded [2424] conformation, whereas a more planar [3333] conformation is observed in the case of the mercury(II) complex. The macrocycle [12]aneNS$_2$O and its structural analogue [12]aneNS$_3$ have then been used as receptor units in the design and synthesis of the new ferrocene-containing redox-active ionophores *N*-ferrocenylmethyl 1-aza-4,10-dithia-7-oxacyclododecane (L^1) and *N*-ferrocenylmethyl 1-aza-4,10,7-trithiacyclododecane (L^2). Electrochemical studies carried out in MeCN in the presence of increasing amounts of Cu^{II}, Zn^{II}, Cd^{II}, Hg^{II}, and Pb^{II} showed that the wave corresponding to the Fc/Fc^+ couple of the uncomplexed ionophores L^1 and L^2 is gradually replaced by a new reversible wave at more positive potentials and corresponding to the Fc/Fc^+ couple of the complexed ionophores. The maximum shift of the ferrocene oxidation wave was found for L^1 in the presence of Zn^{II} (230 mV) and Pb^{II} (220 mV), whereas for L^2 a selective sensing response for Cu^{II} over the other guest metal cations was observed with an oxidation peak shift of 230 mV.

Introduction

The design and development of ion-selective sensors represents an important area of research in supramolecular chemistry. These functionalised molecules generally comprise a receptor unit or guest-binding site which is covalently attached to a signalling unit. The selective host–guest interaction between the target species and the receptor unit causes an easily detectable change in the physical properties of the signalling moiety. In particular, redox-responsive sensors for charged and neutral guests have attracted great attention in the past decade.[1–6] Using the electrochemical technique of cyclic voltammetry, a shift of the redox potential of the active moiety can be easily observed on interaction of the target substrate with the receptor unit of the supramolecular device. The ferrocenyl group is still the most widely used redox probe in electrochemically responsive sensors,[1–10] whereas macrocyclic receptors represent the first choice as guest-binding sites for metal cations due to the great possibility of modulation of host coordination environments that they can offer. Most of the reported ferrocene-based redox-responsive ionophores feature crown ethers[1–6,11–17] or polyaza-macrocycles[1–6,18–20] as receptor units, whereas very few data are available on the electrochemical response of ferrocene-functionalised macrocycles containing S-donor atoms.[21]

We describe here the coordination properties of 1-aza-4,10-dithia-7-oxacyclododecane ([12]aneNS$_2$O) with Cu^{II}, Zn^{II}, Cd^{II}, Hg^{II}, and Pb^{II}. The *N*-ferrocenylmethyl derivatives of [12]aneNS$_2$O (L^1) and 1-aza-4,7,10-trithiacyclododecane ([12]aneNS$_3$) (L^2) have also been synthesised and their electrochemical responses to the above mentioned metal ions investigated by cyclic voltammetry in MeCN solution.

Experimental

All melting points are uncorrected. Microanalytical data were obtained using a Fisons EA CHNS-O instrument operating at 1000 °C. FAB mass spectra were recorded at the Institut für Organische Chemie der Technischen Universität, Braunschweig. ^{1}H and ^{13}C NMR spectra were recorded on a Varian VXR300 spectrometer. UV-visible measurements were carried out at 25 °C using a Varian Model Cary 5 UV-Vis-NIR spectrophotometer. Cyclic voltammetry experiments were recorded at a scan rate of 100 mV s^{-1}, using a conventional three-electrode cell, consisting of a combined working and

† Electronic supplementary information (ESI) available: synthetic details including analytical and spectroscopic data for the isolated complexes. Ortep views of the coordination sphere around the metal centres in **1**, **2** and **5**. See http://www.rsc.org/suppdata/dt/b2/b210806m/

DOI: 10.1039/b210806m

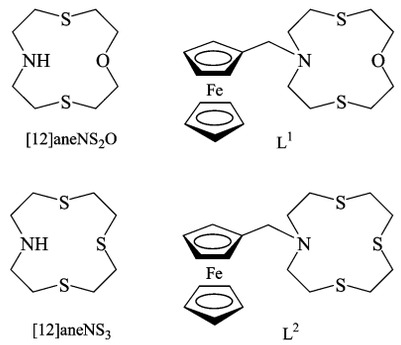

counter platinum electrode and a standard Ag/AgCl (in KCl 3.5 mol dm^{-3}; 0.2223 V at 25 °C) reference electrode. The experiments were performed at 25 °C in anhydrous MeCN. The solutions were about 1×10^{-3} mol dm^{-3} in the electroactive species (L^1 and L^2) with nBu_4NBF_4 (0.1 mol dm^{-3}) as supporting electrolyte. A stream of argon was passed through the solution prior to the scan. For each redox-responsive ionophore (L^1 and L^2), different solutions were prepared containing an increasing amount of the metal guest cation as hydrated perchlorate or tetrafluoroborate salt (molar ratio ranging from 0 to 1 : 1), and the cyclic voltammogram was recorded for each solution. The titration of L^1 and L^2 with $HClO_4$ instead was performed by cautiously adding μL amounts of the concentrated acid (1 mol dm^{-3}) to the MeCN solution of the electroactive species. Data were recorded on a computer controlled EG&G (Princeton Applied Research) potentiostat-galvanostat Model 273 EG&G, using model 270 electrochemical analysis software. Bis(2-mercaptoethyl)ether and di-*tert*-butyl dicarbonate were obtained from Aldrich. The following compounds were prepared according to the reported procedures: *N*-^{t}butoxycarbonyl-bis(2-chloroethyl)amine,[22] 1-aza-4,7,10-trithiacyclododecane ([12]aneNS$_3$),[23] (ferrocenylmethyl)trimethylammonium iodide.[24]

Caution! The Zn^{II}, Hg^{II}, and Pb^{II} complexes of [12]aneNS$_2$O were isolated in the solid state as ClO_4^- salts. We worked with these complexes on a small scale without any incident. Despite these observations, the unpredictable behaviour of ClO_4^- salts necessitate extreme care in handling.

Synthesis of *N*-^{t}butoxycarbonyl 1-aza-4,10-dithia-7-oxacyclododecane (*N*-Boc-[12]aneNS$_2$O)

A solution of bis(2-mercaptoethyl)ether (4.58 g, 0.0331 mol) in anhydrous dmf (250 mL) was added very slowly to a vigorously stirred solution of *N*-^{t}butoxycarbonyl-bis(2-chloroethyl)amine (8 g, 0.0331 mol) and Cs_2CO_3 (16.18 g, 0.050 mol) in anhydrous dmf (800 mL) heated to 60 °C under N_2. After addition was completed, the solution was stirred at 80 °C overnight, Cs_2CO_3 was filtered off and the solvent removed *in vacuo* to yield a yellow oil. The crude product was purified by flash chromatography (silica) using a CH_2Cl_2 : MeOH (97.5 : 2.5 V/V) mixture as eluant to give the desired compound as pale yellow oil (5.35 g, 52.5% yield).^{1}H-NMR (400 MHz, $CDCl_3$): δ_H 1.45 (s, 9 H), 2.73–2.78 (m, 12 H), 3.42–3.45 (m, 4 H). ^{13}C-NMR (300 MHz, $CDCl_3$): δ_C 28.41, 31.98, 32.08, 32.58, 32.73, 46.87, 47.95, 73.11, 73.67, 79.50, 155.38.

Synthesis of 1-aza-4,10-dithia-7-oxacyclododecane ([12]aneNS$_2$O)

Trifluoroacetic acid (25 mL) was added to a solution of *N*-Boc-[12]aneNS$_2$O (5.35 g, 0.0174 mol) in CH_2Cl_2 (25 mL) and the resulting mixture stirred vigorously at room temperature under N_2 for 2 hours. The solvent was removed under reduced pressure and the residue (a pale yellow oil) taken up in water. The pH value was adjusted to 14 by adding 5 M NaOH and the product extracted into CH_2Cl_2. The organic extracts were dried over $MgSO_4$, filtered, and the solvent removed under reduced pressure to give the desired compound as a colourless solid (3.09 g, 86% yield). Mp: 64–65 °C. Elem. Anal. calc. (found for $C_8H_{17}NOS_2$): C, 46.34 (46.28); H, 8.26 (8.56); N, 6.75 (6.60); S, 30.93 (30.31). ^{1}H-NMR (400 MHz, 298 K, $CDCl_3$): δ_H 3.54 (t, J = 5 Hz, 4H), 2.68–2.79 (m, 13H). ^{13}C-NMR (400 MHz, 298 K, $CDCl_3$): δ_C 31.57 (S*C*H$_2$CH$_2$NH), 33.48 (S*C*H$_2$CH$_2$O), 47.21 (HN*C*H$_2$), 70.13 (O*C*H$_2$). Mass Spectrum EI$^+$: *m*/*z* 207 ([$C_8H_{17}NS_2O$]$^+$).

Synthesis of *N*-ferrocenylmethyl 1-aza-4,10-dithia-7-oxacyclododecane (L^1)

A solution of (ferrocenylmethyl)trimethylammonium iodide (1.02 g, 0.0027 mol) in anhydrous MeCN (40 mL) was added dropwise to a refluxing solution of [12]aneNS$_2$O (0.4 g, 0.0019 mol) and K_2CO_3 (2 g, 0.0145 mol) in anhydrous MeCN (40 mL). The resulting orange mixture was stirred overnight at 80 °C. K_2CO_3 was then filtered off and washed with 20 cm^3 of hot MeCN. The solvent was removed under reduced pressure and the residue (an orange oil) was dissolved in CH_2Cl_2 and washed with water. The organic extracts were dried over $MgSO_4$, filtered, and the solvent removed *in vacuo* to yield an orange solid (54% yield) corresponding to L^1HI (**8**), which was purified by flash chromatography (silica) using CH_2Cl_2 : MeOH (70 : 30 V/V) as eluant. Elem. Anal. found (calc. for $C_{19}H_{28}FeINOS_2$): C, 42.77 (42.79); H, 5.28 (5.29); N, 2.58 (2.63); S, 12.09 (12.02)%. **8** (0.40 g) was then washed with 5 M KOH, extracted in CH_2Cl_2, and dried over $MgSO_4$. The solvent was removed *in vacuo* to yield 0.23 g (75% yield) of pure product L^1. Mp: 98 °C. Elem. Anal. found (calc. for $C_{19}H_{27}FeNOS_2$): C, 56.15 (56.29); H, 6.76 (6.71); N, 3.60 (3.45); S, 16.26 (15.82)%. ^{1}H-NMR (300 MHz, $CDCl_3$): δ_H 2.68 (t, J = 3.6, 4 H), 2.76–2.81 (m, 8 H), 3.50 (s, 2 H), 3.73 (t, J = 3.6, 4 H), 4.07 (s, 5 H), 4.138–4.139 (m, 4 H). ^{13}C-NMR (300 MHz, $CDCl_3$): δ_C 27.96 (S*C*H$_2$CH$_2$N), 30.35 (S*C*H$_2$CH$_2$O), 50.79 (N*C*H$_2$CH$_2$S), 55.13 (N*C*H$_2$Fc), 67.93, 68.38, 69.85, 74.37 (O*C*H$_2$), 83.69. UV-vis spectrum (MeCN): λ_{max} = 325 (ε_{max} = 75), 438 nm (113 dm^3 mol^{-1} cm^{-1}).

Synthesis of *N*-ferrocenylmethyl 1-aza-4,10,7-trithiacyclododecane (L^2)

A solution of (ferrocenylmethyl)trimethylammonium iodide (1.2 g, 0.0031 mol) in anhydrous MeCN (50 mL) was added dropwise to a refluxing solution of [12]aneNS$_3$ (0.5 g, 0.0022 mol) and K_2CO_3 (1.73 g, 0.0125 mol) in anhydrous MeCN (50 mL). The resulting orange solution was stirred overnight. K_2CO_3 was filtered off and the solvent was removed under reduced pressure. The residue (an orange solid) was taken up in CH_2Cl_2 and washed with water. The organic extracts were dried over $MgSO_4$, filtered, and the solvent removed under reduced pressure to yield an orange solid. The product was purified by flash chromatography (silica) using CH_2Cl_2 : MeOH (70 : 30 V/V) as eluant (0.723 g, 78% yield). Mp: 111 °C. Elem. Anal. found (calc. for $C_{19}H_{27}FeNS_3$): C, 53.96 (54.15); H, 6.26 (6.46); N, 3.41 (3.32); S, 22.82 (22.82)%. ^{1}H-NMR (400 MHz, $CDCl_3$): δ_H 2.54–2.57 (m, 4 H), 2.65–2.67 (m, 4 H), 2.77–2.79 (m, 8 H), 3.52 (s, 2H), 4.07 (s, 5 H), 4.09–4.11 (m, 4 H). ^{13}C-NMR (400 MHz, $CDCl_3$): δ_C 26.84 (S*C*H$_2$CH$_2$N), 28.40 and 29.51 (S*C*H$_2$*C*H$_2$S), 52.40 (SCH$_2$*C*H$_2$N), 54.01 (N*C*H$_2$Fc), 67.99, 68.37, 69.80, 82.15. UV-vis spectrum (MeCN): λ_{max} = 324 (ε_{max} = 90), 435 nm (110 dm^3 mol^{-1} cm^{-1}).

Synthesis of the complexes [Cu([12]aneNS$_2$O)Cl$_2$] (1), [Cu([12]aneNS$_2$O)Br$_2$] (2), [Cu([12]aneNS$_2$O)(NO$_3$)$_2$] (3), [Zn([12]aneNS$_2$O)](ClO$_4$)$_2$ (4), [Cd([12]aneNS$_2$O)(NO$_3$)$_2$] (5), [Hg([12]aneNS$_2$O)MeCN](ClO$_4$)$_2$ (6), [Pb([12]aneNS$_2$O)](ClO$_4$)$_2$ (7), and [Cd(L^1)(NO$_3$)$_2$]·Et$_2$O (9)

All complexes have been synthesised by following a standard procedure which includes the mixing of the appropriate metal salt and the ligand ([12]aneNS$_2$O or L^1) in 1 : 1 molar ratio in

MeCN or MeOH and the isolation of the product as crystals or powder from the reaction mixture stirred for a few hours at room temperature by diffusion of vapours of Et_2O. Synthetic details including analytical and spectroscopic data for the isolated complexes have been deposited as Electronic Supplementary Information (ESI)† and they are consistent with the formulation given for the complexes. As a representative example the full synthetic procedure for the preparation of **9** is here reported: $Cd(NO_3)_2{\cdot}4H_2O$ (10.2 mg, 0.0493 mmol) was added to a solution of *N*-ferrocenylmethyl-[12]aneNS$_2$O (L^1) (20 mg, 0.0493 mmol) in MeCN (5 mL). The mixture was stirred at room temperature for four hours. The solvent was partially removed under reduced pressure and the product crystallised by diffusion of Et_2O vapour into the remaining solution. Yellow crystals were obtained (18.82 mg, 61% yield). Mp: 248–250 °C. Elem. Anal. found (calc. for $C_{23}H_{37}CdFeN_3O_8S_2$): C, 38.62 (38.58); H, 5.08 (5.21); N, 5.58 (5.87); S, 8.51 (8.96)%. UV-vis spectrum (MeCN): λ_{max} = 438 (ε_{max} 105 dm^3 mol^{-1} cm^{-1}).

Potentiometric measurements

All pH metric measurements were carried out in degassed 0.1 mol dm^{-3} NMe_4NO_3 water solutions, at 298.1 K, using the equipment and procedure described elsewhere.[25] The combined Ingold 405 S7/120 electrode was calibrated as a hydrogen concentration probe by titrating amounts of HCl with CO_2-free NMe_4OH solutions and determining the equivalent point by Gran's method[26] which allows one to determine the standard potential $E°$, and the ionic product of water (pK_w = 13.83(1) at 298.1 K in 0.1 mol dm^{-3} NMe_4NO_3). 0.5×10^{-3}–1×10^{-3} mol dm^{-3} ligands and metal ion concentrations were employed in the potentiometric measurements, performing three titration experiments (about 100 data points each) in the pH range 2.5–11. The relevant e.m.f. data were treated by means of the computer program HYPERQUAD.[27]

Crystallography

Crystal data and refinement details of all structure determinations appear in Table 1. Only special features of the analyses are pointed out here. Single crystal data collections for [Cu([12]aneNS$_2$O)Cl$_2$](**1**),[Cu([12]aneNS$_2$O)Br$_2$](**2**),[Cd([12]aneNS$_2$O)(NO$_3$)$_2$] (**5**) and [Hg([12]aneNS$_2$O)MeCN](ClO$_4$)$_2$ (**6**) were performed on a CAD-4 diffractometer using ω scans. For [Cu([12]aneNS$_2$O)(NO$_3$)$_2$] (**3**), L^1HI (**8**) and [Cd(L^1)(NO$_3$)$_2$]·Et$_2$O (**9**) data were acquired on a SMART CCD diffractometer using ω scans. All datasets were corrected for Lorentz-polarization effects and for absorption as specified in Table 1. The structures were solved by direct methods using the SHELXS program[29] followed by difference Fourier synthesis. All non-H atoms were refined anisotropically and H atoms were introduced at calculated positions and thereafter incorporated into a riding model with U_{iso}(H) = 1.2U_{eq}(C). The structures were developed by alternating cycles of least-squares refinements on F^2 and ΔF synthesis.[30] In **3** one of the NO_3^- ion in the asymmetric unit was found to be disordered. The disorder in the NO_3^- ion was modelled by two equally occupied sites for each O atom. The two components of the disordered NO_3^- ion coincident at the nitrogen atom were refined isotropically with restraints to impose trigonal planar geometry on each. In **4**, some atoms of the macrocycle ring (see Fig. 4) display slightly high displacement parameters which may be indicative of partial disorder due to the presence of similar but different conformations. Any attempt to split each of these atoms into two components offered no advantage. In **8**, the carbon atoms in one of the cyclopentadienyl rings in the ferrocene unit were found to be disordered and the disorder was modelled over two sites with occupancy factor 0.60 for the major components. ORTEP views of the coordination sphere around the metal

Table 1 Crystallographic data for [Cu([12]aneNS$_2$O)Cl$_2$](**1**), [Cu([12]aneNS$_2$O)Br$_2$](**2**),[Cu([12]aneNS$_2$O)(NO$_3$)$_2$](**3**),[Cd([12]aneNS$_2$O)(NO$_3$)$_2$](**5**),[Hg([12]aneNS$_2$O)MeCN](ClO$_4$)$_2$(**6**), L^1HI (**8**), [Cd(L^1)(NO$_3$)$_2$]·Et$_2$O(**9**)

Compound	**1**	**2**	**3**	**5**	**6**	**8**	**9**
Formula	$C_8H_{17}Cl_2CuNOS_2$	$C_8H_{17}Br_2CuNOS_2$	$C_8H_{17}CuN_3O_7S_2$	$C_8H_{17}CdN_3O_7S_2$	$C_{10}H_{20}Cl_2HgN_2O_9S_2$	$C_{19}H_{28}FeINOS_2$	$C_{23}H_{37}CdFeN_3O_8S_2$
Crystal system	Monoclinic	Monoclinic	Monoclinic	Orthorhombic	Orthorhombic	Orthorhombic	Orthorhombic
Space group	$P2_1/n$ (no. 14)	$P2_1/n$ (no. 14)	$P2_1/c$ (no. 14)	$P2_12_12_1$ (no. 19)	*Pbca* (no. 61)	$Pna2_1$ (no. 33)	$P2_12_12_1$ (no. 19)
M	341.79	430.71	394.91	443.77	647.89	533.29	715.93
a/Å	8.744(3)	9.708(3)	14.763(1)	8.950(2)	7.940(3)	11.474(1)	12.1242(9)
b/Å	11.315(3)	10.823(4)	14.952(1)	11.980(3)	15.503(2)	17.142(1)	13.6318(10)
c/Å	13.913(3)	13.658(5)	14.747(1)	14.746(4)	31.611(4)	10.771(1)	18.1656(14)
β/°	91.81(2)	105.76(3)	111.32(1)				
V/Å^3	1375.9(7)	1381.0(8)	3032.4(4)	1581.1(7)	3891.1(16)	2118.5(3)	3002.3(4)
Z	4	4	8	4	8	4	4
T/K	293(2)	293(2)	293(2)	293(2)	293(2)	293(2)	293(2)
D_c/g cm^{-3}	1.650	2.072	1.730	1.864	2.212	1.672	1.584
μ/mm^{-1}	2.254	7.646	1.750	1.678	8.446	2.374	1.378
Unique Reflections	2407	2427	5339	3436	3368	3762	5895
Observed Reflections [$I > 2\sigma(I)$]	1866	1426	3655	2892	1687	2354	4522
Absorption correction	ψ-scans	ψ-scans	SADABS[28]	ψ-scans	ψ-scans	SADABS[28]	SADABS[28]
T_{min}, T_{max}	0.94, 1.00	0.51, 1.00	0.81, 1.00	0.93, 1.00	0.93, 1.00	0.90, 1.00	0.80, 1.00
R_1	0.0230	0.0316	0.0356	0.0226	0.0415	0.0246	0.0350
wR_2 [all data]	0.0603	0.0737	0.0888	0.0564	0.1246	0.0485	0.1003

Table 2 Protonation constant of [12]aneNS$_2$O (L) and stability constants (log$K$) of its metal complexes (NMe_4NO_3 0.1 mol dm^{-3}, 298.1 K)

Reaction	log$K$	Reaction	log$K$
$L + H^+ \rightleftharpoons HL^+$	8.73(4)	$Cd^{II} + L \rightleftharpoons [CdL]^{2+}$	7.90(5)
$Cu^{II} + L \rightleftharpoons [CuL]^{2+}$	8.13(4)	$Hg^{II} + L \rightleftharpoons [HgL]^{2+}$	8.65(4)
$[CuL]^{2+} + OH^- \rightleftharpoons [CuL(OH)]^+$	6.29(9)		
$[CuL(OH)]^+ + OH^- \rightleftharpoons [CuL(OH)_2]$	3.30(1)	$Pb^{II} + L \rightleftharpoons [PbL]^{2+}$	4.20(9)
		$[PbL]^{2+} + OH^- \rightleftharpoons [PbL(OH)]^+$	5.94(2)

centres in **1**, **2** and **5** have been deposited as Electronic Supplementary Information (ESI). †

CCDC reference numbers 196822–196828.

See http://www.rsc.org/suppdata/dt/b2/b210806m/ for crystallographic data in CIF or other electronic format.

Results and discussion

Synthesis of [12]aneNS$_2$O and its coordination properties towards Cu^{II}, Zn^{II}, Cd^{II}, Hg^{II}, and Pb^{II}

The coordination properties of 12-membered macrocyclic ligands featuring four donor atoms, such as 1,4,7,10-tetraazacyclododecane ([12]aneN$_4$), 1,4,7,10-tetraoxacyclododecane ([12]aneO$_4$), 1,4,7,10-tetrathiacyclododecane ([12]aneS$_4$), and mixed N/O- and N/S-donor analogues have been extensively studied both in solution and in the solid state.[31–37] Some of these macrocyclic ligands (in particular [12]aneNO$_3$ and [12]aneN$_2$O$_2$) have also been successfully used as receptor units in redox-responsive sensors.[11,15] Instead, due to synthetic difficulties encountered in their preparation, far less work has been done on 12-membered macrocyclic ligands containing three different donors.[38–41] The choice of [12]aneNS$_2$O for the construction of a ferrocene-based redox-responsive ionophore for transition metal ions was mainly determined by the presence in its donor set of both soft (S) and hard (N, O) donors which should ensure strong complexation to a great variety of metal ions.

[12]aneNS$_2$O has been synthesised by performing the cyclization reaction between Boc-N(CH$_2$CH$_2$Cl)$_2$ and O(CH$_2$CH$_2$SH)$_2$ in dmf under high dilution conditions according to the procedure reported by Reedijk *et al.* for the preparation of mixed N/S/O macrocycles.[23] The Boc-protected [12]aneNS$_2$O macrocycle can be deprotected with 50% trifluoroacetic acid-solution in CH$_2$Cl$_2$ at room temperature to give the desired compound with an overall and reproducible yield of 45%. With respect to other procedures reported in the literature for the same macrocycle,[40,41] this one offers the advantage of an easier deprotection step of the nitrogen atom after the cyclization reaction and a consequent higher overall yield.

Protonation for [12]aneNS$_2$O and complex formation with Cu^{II}, Zn^{II}, Cd^{II}, Hg^{II}, and Pb^{II} have been investigated by means of potentiometric measurements in aqueous solutions (NMe_4NO_3 0.1 mol dm^{-3}, 298.1 K) in the pH range 2.5–11 [Cu^{II} and Pb^{II}] or 2.5–7 [Cd^{II} and Hg^{II}]. In the case of Cd^{II} and Hg^{II}, precipitation at slightly alkaline pHs of hydroxo-complexes does not allow the study of these systems in the alkaline pH region. The stability constant of the Zn^{II} complex is too low to be determined, and precipitation of Zn^{II} hydroxide takes place at slightly acidic pH values.

Protonation constant, formed complexes, and corresponding stability constants are reported in Table 2, while Fig. 1 reports the distribution diagram for the Cu^{II}/[12]aneNS$_2$O, Hg^{II}/[12]aneNS$_2$O and Pb^{II}/[12]aneNS$_2$O systems. For the Cd^{II}/[12]aneNS$_2$O system the distribution diagram resembles that obtained for the Hg^{II}/[12]aneNS$_2$O system. The protonation constant value falls in the range usually found for secondary amines.

As shown in Fig. 1a, Cu^{II} complexation occurs at slightly acidic pH values, with the formation of the [Cu([12]aneNS$_2$O)]$^{2+}$ species; deprotonation of water molecules at alkaline pH values gives the mono- and dihydroxo-complexes [Cu([12]aneNS$_2$O)(OH)]$^+$ and [Cu([12]aneNS$_2$O)(OH)$_2$]. Interestingly, the stability constant of the [Cu([12]aneNS$_2$O)]$^{2+}$ complex is lower than that found for the macrocycle *trans*-[12]aneN$_2$S$_2$ (log$K$ = 12.02),[42] due to the replacement of a nitrogen donor with a hard oxygen atom in [12]aneNS$_2$O. At the same time, the present [Cu([12]aneNS$_2$O)]$^{2+}$ complex shows a higher tendency to form a monohydroxo-complex than *trans*-[12]aneN$_2$S$_2$ (log$K$ = 6.29 *vs.* 4.76 for the equilibrium $[CuL]^{2+} + OH^- \rightleftharpoons [CuL(OH)]^+$, L = [12]aneNS$_2$O and [12]aneN$_2S_2$, respectively), once more due to the reduced σ-donating ability of the oxygen donor in [12]aneNS$_2$O, which leads to a decrease in electron density at the metal centre and an increase in the acidity of the coordinated water molecules with respect to the Cu(II) complex with [12]aneN$_2$S$_2$.[42]

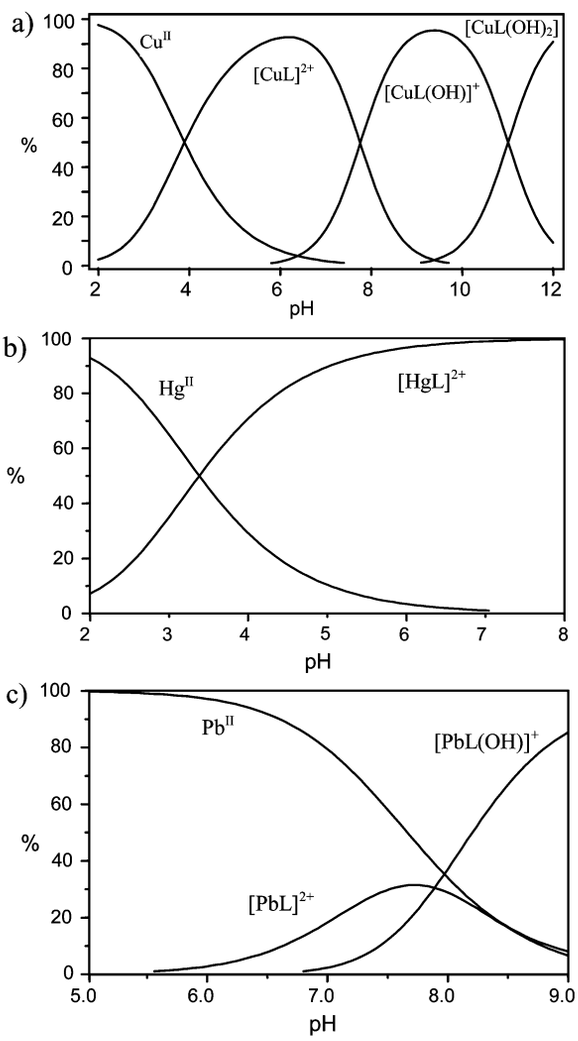

Fig. 1 Distribution diagrams for the systems Cu^{II}/L (a), Hg^{II}/L (b) and Pb^{II}/L (c) (L = [12]aneNS$_2$O; [M^{II}] = [L] = 1 × 10^{-3} mol dm^{-3}, 298.1 K; I = 0.1 mol dm^{-3}).

Similarly to Cu^{II}, Hg^{II} and Cd^{II} complexation takes place above pH 3, as shown in Fig. 1b for Hg^{II}. In the case of Pb^{II}, the

Table 3 Formation constants (log$K$) for 1 : 1 complexes between Cu^{II}, Zn^{II}, Cd^{II}, Hg^{II} and Pb^{II} and mixed N/S/O-donor tetradentate 12-membered macrocycles[a]

	Cu^{II}	Zn^{II}	Cd^{II}	Hg^{II}	Pb^{II}
cis-[12]aneN_2S_2	14.21(2)[42b]				
	13.95[43c]				
trans-[12]aneN_2S_2	12.02(2)[42b]				
[12]aneN_3S	17.98(5)[44d]	9.58(7)[36]	9.91(4)[36]	24.32(5)[44d]	10.96(11)[36]
	17.85[36]				
[12]aneN_4	24.80[45d]	16.2(2)[46d]	14.3(2)[46d]	25.50[47d]	15.9(2)[46d]
	23.29(6)[48e]				
[12]aneN_3O	15.63(1)[35]	10.43(7)[35]	10.69(1)[35]	14.83(7)[36]	11.54(1)[34,35]
	15.85(2)[34]	10.53(1)[34]	10.78(1)[34]		
cis-[12]aneN_2O_2	8.7(1)[34]				6.3(1)[34]
trans-[12]aneN_2O_2	7.92(2)[49]	6.51(6)[49]	6.55(8)[49]		6.37(2)[49]
[12]aneNO_3		3.7(1)[50f]	<4.5[50f]	>11[50f]	4.1[51]
trans-[12]aneN_2SO				10.5[39]	6.6[39]
trans-[12]aneNO_2S					4.2[39]
trans-[12]aneNS_2O	8.13(4)		7.90(5)	8.65(4)	4.20(9)

[a] Where no indications have been given, the reported formation constants have been determined potentiometrically in water solution at 25 °C, fixing the ionic strength (I) at 0.1 mol dm^{-3}. [b] I = 0.5 mol dm^{-3}. [c] T = 20 °C, I = 0.2 mol dm^{-3}. [d] The formation constant was determined by the anodic polarographic technique, I = 0.2 mol dm^{-3}. [e] I = 0.5 mol dm^{-3}. [f] Since the formation constant was determined in 95% vol/vol MeOH/H_2O, the comparison with the formation constants for the other macrocycles can only be qualitative.

formation of the $[Pb([12]aneNS_2O)]^{2+}$ complex, above pH 6 (Fig. 1c), is followed by deprotonation at almost neutral pH of a metal-coordinated water molecule to give the $[Pb([12]aneNS_2O)(OH)]^{+}$ complex. Table 3 collects the 1 : 1 complex formation constants reported in the literature of N,S,O-mixed donor 12-membered tetradentate macrocycles with Cu^{II}, Zn^{II}, Cd^{II}, Hg^{II}, and Pb^{II}. An N>O>S donor affinity trend can be easily recognised for Zn^{II}, Pb^{II}, and Cd^{II}, although in some cases the discrimination of oxygen over sulfur is small [compare the formation constants for the 1 : 1 complexes of Pb^{II} with the couples of ligands [12]aneNO_2S/[12]aneNS_2O, [12]aneN_2SO/[12]aneN_2O_2 and [12]aneN_3O/[12]aneN_3S; and of Cd^{II} and Zn^{II} with the couple [12]aneN_3O/[12]aneN_3S]. For Cu^{II} and Hg^{II} the donor affinity trend appears to be N>S>O with a pronounced differentiation between sulfur and oxygen, especially for Hg^{II}. The presence of two soft sulfur atoms as donors in [12]aneNS_2O can therefore explain the observed increasing binding ability starting from Zn^{II}, which is not complexed in our experimental conditions, as far as Pb^{II} (log$K$ = 4.20), Cd^{II} (log$K$ = 7.90), Cu^{II} (log$K$ = 8.13) and Hg^{II} (log$K$ = 8.65), which actually forms the most stable complex.

It is well known that 12-membered tetradentate macrocycles such as [12]aneN_4 cannot usually host divalent transition metal ions within their cavity to give coplanarity between the four donor atoms and the guest metal. Due to the short ethano bridges between the donor atoms, these macrocycles are generally too small to act as planar tetradentate ligands without being very strained, and therefore conformational changes are normally required for the ring cavity upon complexation. In order to better understand the chelating ability of [12]aneNS_2O, the 1 : 1 complexes $[Cu([12]aneNS_2O)Cl_2]$ (**1**), $[Cu([12]aneNS_2O)Br_2]$ (**2**), $[Cu([12]aneNS_2O)(NO_3)_2]$ (**3**), $[Zn([12]aneNS_2O)](ClO_4)_2$ (**4**), $[Cd([12]aneNS_2O)(NO_3)_2]$ (**5**), $[Hg([12]aneNS_2O)MeCN](ClO_4)_2$ (**6**), and $[Pb([12]aneNS_2O)](ClO_4)_2$ (**7**) have been prepared directly by treating [12]aneNS_2O with the appropriate metal salt in MeCN (see Experimental), of which complexes **1**, **2**, **3**, **5**, and **6** have also been characterised by X-ray crystal structure determination. Figs. 2 and 3 show the coordination sphere around the metal centres in **3** and **6**, and Table 4 summarizes selected bond distances and angles for all structurally characterised complexes. In **1**, **2**, and **3** the macrocyclic ligand adopts a folded conformation resembling an open book with the "fold" along the S(4)–Cu–S(10) direction and an N(1)–Cu–O(7) angle very close to 90° [85.05(7)–91.49(10)°]. The two *cis*-positions of a pseudo-octahedral coordination sphere around the metal centre left free

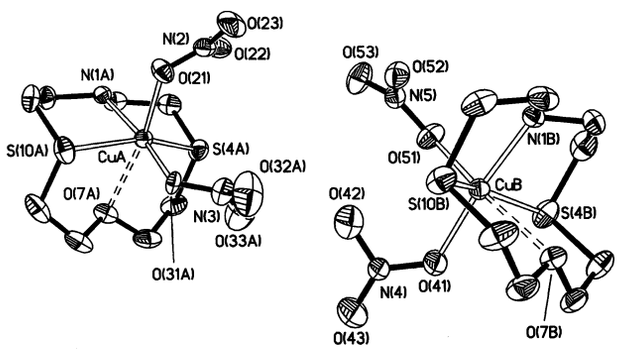

Fig. 2 ORTEP view of the two independent molecules in the asymmetric unit of $[Cu([12]aneNS_2O)(NO_3)_2]$ (**3**) with the adopted numbering scheme. Displacement ellipsoids are drawn at 30% probability and hydrogen atoms have been omitted for clarity. Only one component of the disordered $N(3)O_3$ ion is shown.

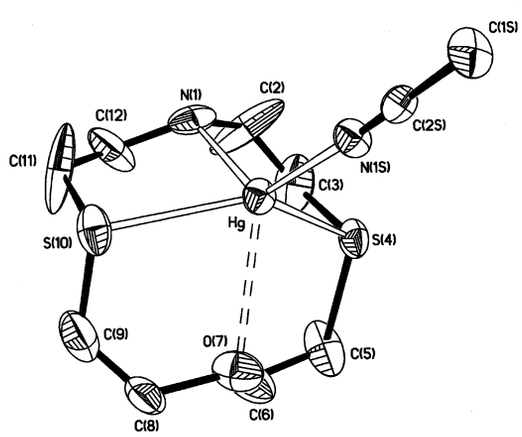

Fig. 3 ORTEP view of the complex cation $[Hg([12]aneNS_2O)MeCN]^{2+}$ in **6** with the adopted numbering scheme. Displacement ellipsoids are drawn at 30% probability. Hydrogen atoms and ClO_4^- counter anions have been omitted for clarity.

by the macrocylic ligand are occupied by two Cl^- (**1**), Br^- (**2**) and monodentate NO_3^- (**3**) ligands (see Fig. 2 for **3**). The Cu^{II} ions are displaced from 0.288 (**1**) to 0.226 (asymmetric unit A in **3**) Å out of the equatorial mean planes defined by the atoms N(1), S(4), S(10) and X(1) {Cl(1) (**1**), Br(1) (**2**) and O(31A)NO_2 [O(41)NO_2] (**3**)} towards the apical X(2) atom {Cl(2) (**1**), Br(2) (**2**) and O(21)NO_2 [O(51)NO_2] (**3**), see Table 4} and away from

Table 4 Selected bond distances (Å) and angles (°) for [Cu([12]aneNS$_2$O)Cl$_2$] (**1**), [Cu([12]aneNS$_2$O)Br$_2$] (**2**), [Cu([12]aneNS$_2$O)(NO$_3$)$_2$] (**3**),[a] [Cd([12]aneNS$_2$O)(NO$_3$)$_2$] (**5**), [Hg([12]aneNS$_2$O)MeCN](ClO$_4$)$_2$ (**6**), and [Cd(L^1)(NO$_3$)$_2$]·Et$_2$O (**9**)[b]

	1	**2**	**3**	**5**[c]	**6**	**9**[c]
M–N(1)	2.029(2)	2.044(4)	1.995(3) [2.000(3)]	2.326(4)	2.389(13)	2.436(4)
M–S(4)	2.4087(10)	2.369(2)	2.3459(11) [2.4406(11)]	2.6635(12)	2.550(3)	2.639(2)
M–S(10)	2.4139(11)	2.370(2)	2.4054(11) [2.3620(11)]	2.6697(11)	2.521(4)	2.655(2)
M–O(7)	2.595(2)	2.587(4)	2.455(3) [2.402(2)]	2.561(3)	2.748(10)	2.564(4)
M–X(1)	2.2530(8)	2.4125(12)	1.922(6) [1.972(3)]	2.381(4) [2.530(3)]	2.187(10)	2.998(10) [2.290(5)]
M–X(2)	2.4716(10)	2.6607(12)	2.242(3) [2.268(3)]	2.578(4) [2.391(4)]		2.396(4) [2.541(5)]
N(1)–M–S(4)	86.63(7)	86.80(13)	87.86(8) [87.39(9)]	80.59(10)	82.0(4)	81.36(11)
N(1)–M–S(10)	86.69(7)	87.21(13)	87.78(9) [88.02(9)]	79.76(9)	81.2(4)	81.25(11)
N(1)–M–O(7)	85.05(7)	86.28(15)	90.83(11) [91.49(10)]	81.50(12)	111.2(4)	82.93(13)
N(1)–M–X(1)	177.31(7)	176.16(13)	168.9(2) [173.05(12)	98.01(15) [83.76(12)]	125.9(4)	150.7(2) [165.5(2)]
N(1)–M–X(2)	86.56(6)	86.81(12)	91.28(11) [88.70(11)]	153.91(13) [156.33(13)]		91.9(2) [91.00(14)]
S(4)–M–S(10)	154.08(3)	155.14(6)	158.08(4) [158.03(4)]	141.39(4)	133.72(12)	143.03(6)
S(4)–M–O(7)	77.18(5)	78.63(10)	80.13(8) [78.40(7)]	72.29(8)	72.7(2)	72.81(12)
S(4)–M–X(1)	92.77(3)	90.29(5)	103.0(2) [85.98(10)]	133.54(10) [83.05(9)]	106.7(3)	72.5(2) [112.9(2)]
S(4)–M–X(2)	103.90(3)	107.79(5)	115.27(8) [84.52(7)]	109.06(11) [82.23(11)]		84.26(13) [134.52(10)]
S(10)–M–O(7)	77.31(4)	76.91(10)	78.46(8) [80.25(7)]	72.17(8)	73.9(3)	72.84(12)
S(10)–M–X(1)	92.74(3)	94.41(5)	81.2(2) [97.37(10)]	82.10(10) [127.02(9)]	118.0(3)	112.2(2) [85.4(2)]
S(10)–M–X(2)	100.66(3)	95.94(5)	86.30(8) [116.84(7)]	78.06(10) [123.45(10)]		128.68(13) [78.09(10)]
O(7)–M–X(1)	92.26(4)	90.70(9)	88.5(3) [85.14(11)]	153.97(12) [152.97(11)]	122.4(4)	77.1(3) [98.5(2)]
O(7)–M–X(2)	171.46(4)	170.28(9)	164.52(10) [162.90(9)]	78.77(13) [108.52(13)]		157.0(2) [150.9(2)]
X(1)–M–X(2)	96.13(3)	96.47(3)	86.5(3) [92.75(12)]	50.92(12) [48.83(12)][d]		41.7(2) [51.1(12)][d]

[a] Two molecules of [Cu([12]aneNS$_2$O)(NO$_3$)$_2$] are present in the asymmetric unit of **3**. [b] X(1) = Cl(1) (**1**), Br(1) (**2**), O(31A)NO$_2$ [O(41)NO$_2$] (**3**), MeCN (**6**), N(2)O$_3$ (**5** and **9**); X(2) = Cl(2) (**1**), Br(2) (**2**), O(21)NO$_2$ [O(51)NO$_2$] (**3**), N(3)O$_3$ (**5** and **9**). [c] Where two values are reported, the first refers to bond distances and angles involving O(21) or O(31), and the second to bond distances and angles involving O(22) or (32). [d] X(1)–M–X(2) = O(21)–Cd–O(22) [O(31)–Cd–O(32)].

O(7) [O(7)–Cu–X(2) 162.90(9)–171.46(4)°] which provides the longest Cu–donor interaction.

A similar folded conformation is adopted by [12]aneNS$_2$O in the [Cd([12]aneNS$_2$O)(NO$_3$)$_2$] (**5**) complex. In this case, the N(1)–Cd–O(7) "folding" angle is only 81.50(12)° (Table 4) presumably due both to the larger size of the Cd^{II} ion and to the steric hindrance of the two bidentate nitrate ions, which if regarded as single ligands can be considered to occupy the *cis*-positions left free by the macrocyclic ligand of a formal *pseudo*-octahedral coordination sphere around the metal centre. In fact, compared to Cu^{II} in the complexes **1**, **2**, and **3**, the Cd^{II} ion in **5** is much more displaced out of the ring cavity of [12]aneNS$_2$O in agreement with the lower value observed for the S(4)–Cd–S(10) angle [141.39(4)°], but it forms a Cd–O(7) bond [2.561(3) Å] which is shorter than the Cd–S bonds [2.6635(12), 2.6697(11) Å]. Interestingly the folded [2424] conformation adopted by [12]aneNS$_2$O in both the Cu^{II} and Cd^{II} complexes is such that all torsion angles at the C–N(1) and C–O(7) bonds assume *anti* arrangements with absolute values of the angles ranging from 169.0(5) to 179.7(4)° for the placements at the C–O(7) bonds, and from 164.7(5) to 175.2(3)° for those at the C–N(1) bonds. One of each pair of torsion angles about the C–S bonds is *gauche* [60.3(4)–68.9(5)°], the other torsion angle ranges from 114.3(4) to 125.4(4)°, whereas a *gauche* disposition is preferred at the C–C bonds [47.8(6)–62.4(3)°].

A more planar [3333] conformation is adopted by [12]aneNS$_2$O in the [Hg([12]aneNS$_2$O)MeCN]$^{2+}$ complex cation in **6** (Fig. 3, Table 4) presumably due to the increased metal ion radius and the reduced coordination number for it. In fact, essentially the Hg^{II} ion has a distorted tetrahedral geometry, since it is coordinated to the two S atoms of the macrocycle and two N-donors, one from the macrocyclic framework and an acetonitrile molecule, respectively. A weak bond interaction is present between the metal centre and O(7) [2.748(10) Å]. This interaction is slightly longer than those observed in [Hg([12]aneNSO$_2$)(NO$_3$)$_2$] (2.722(13), 2.654(13) Å)[37] and [Hg([12]aneN$_2$SO)(NO$_3$)$_2$] (2.63(1) Å)[39] but still shorter than the sum of the van der Waals radii of mercury(II) and oxygen.[52]

Synthesis of L^1 and L^2 and electrochemical behaviour of these new redox-active receptors in the presence of Cu^{II}, Zn^{II}, Cd^{II}, Hg^{II}, and Pb^{II}

Compound L^1 was prepared following a well established procedure for the introduction of ferrocenylmethyl frameworks to secondary amines, *i.e.* by reaction of [12]aneNS$_2$O with the salt (ferrocenylmethyl)trimethylammonium iodide[24] in MeCN in the presence of anhydrous K$_2$CO$_3$.[10,13,15,19,21] In this case the product obtained after standard work-up and purification by flash-chromatography was not L^1 but its iodide salt L^{1}HI (**8**). A subsequent treatment of this salt with concentrated KOH and extraction with CH$_2$Cl$_2$ were necessary to obtain the desired neutral compound L^1. Single crystals of the salt L^{1}HI were grown by diffusion of Et$_2$O vapour into a MeCN solution. An X-ray diffraction analysis (Fig. 4a) reveals that the macrocyclic framework adopts a folded [2424] conformation very similar to that observed for [12]aneNS$_2$O in the complexes **1**–**3**, and **5**, with the same sequence of torsion angles around the C–E (E = S, O, N) and C–C bonds. Presumably, in this case the conformation is determined by the intramolecular NH ··· O hydrogen bond [N(1)H(1) ··· O(7) 2.29(4), N(1) ··· O(7) 2.990(4) Å, N–H ··· O 133.0(9)°].

Unfortunately, the insolubility of either L^{1}HI or L^1 in water has prevented a potentiometric study of the coordination properties towards Cu^{II}, Zn^{II}, Cd^{II}, Hg^{II}, and Pb^{II} of this new redox-active receptor.

The cadmium complex of L^1 was obtained by reaction with cadmium nitrate in MeCN followed by diffusion of Et$_2$O vapour into the reaction mixture. An X-ray diffraction analysis on a single crystal confirms the formation of the [Cd(L^1)(NO$_3$)$_2$]·Et$_2$O (**9**) complex (Fig. 4b, Table 4). The coordination environment around the metal centre resembles that observed in complex **5** with four positions occupied by the NS$_2$O-donor set of the macrocyclic framework, which is folded over the S–Cd–S axis [S(4)–Cd–S(10) 143.03(6), [N(1)–Cd–O(7) 82.93(13)°] and the remaining sites taken up respectively by a bidentate and an essentially monodentate nitrate ion.

The electrochemical response of L^1 to the presence of Cu^{II}, Zn^{II}, Cd^{II}, Hg^{II}, or Pb^{II} as guest metal cation species has been

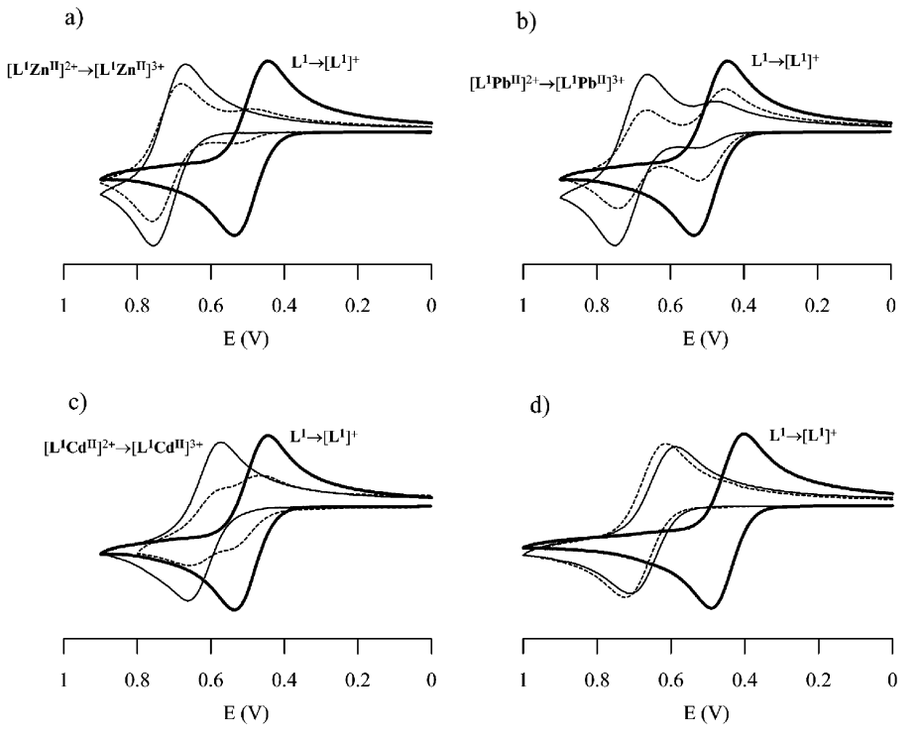

Fig. 5 Cyclic voltammetry in acetonitrile solution of: (a) $L^1 + Zn^{II}$; (b) $L^1 + Pb^{II}$; (c) $L^1 + Cd^{II}$ and (d) $L^1 + H^+$. The full bold line refers to L^1, the dotted line to L^1 + 0.5 equivalents of the guest cations, and the full thin line to L^1 + 1 equivalent of guest cations.

investigated by cyclic voltammetry (CV) in MeCN solution at 25 °C. For comparison we have also studied the electrochemical response towards the same set of metal cations of L^2, which was prepared starting from [12]aneNS$_3$[23] and following the same synthetic route adopted for the synthesis of L^1. In this way, seeking a selective sensing function, we wanted to understand the effect of the host–guest interaction on the oxidation potential of the ferrocene redox-antenna upon replacing an O-donor with an S-donor in the 12-membered host macrocyclic framework of L^1.

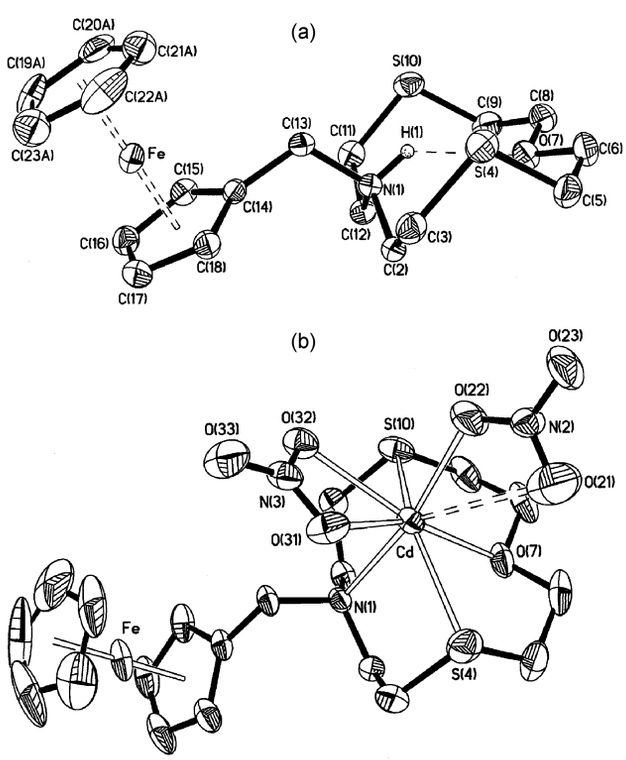

Fig. 4 ORTEP view of the cation $[L^1H]^+$ in **8** (a) and of the complex $[Cd(L^1)(NO_3)_2]$ in **9** (b) with the adopted numbering scheme. Displacement ellipsoids are drawn at 30% probability. Hydrogen atoms and the co-crystallised Et_2O molecule in **9** have been omitted for clarity.

Cyclic voltammetry in MeCN of the free ligand L^1 as expected reveals a one-electron reversible oxidation wave at $E_{1/2}$ = 490 mV *vs.* Ag/AgCl, corresponding to the Fc/Fc$^+$ redox couple. This wave is gradually replaced by a new reversible wave at more positive potentials upon addition of increasing amounts of Cu^{II}, Zn^{II}, Cd^{II}, Hg^{II}, or Pb^{II} as guest metal cation species (see Fig. 5). The anodically shifted electrochemical wave corresponds to the Fc/Fc$^+$ redox couple of the $[L^1M^{II}]^{2+}$ species. Its position with respect to the wave corresponding to uncomplexed L^1 reflects a less favourable oxidation process for the Fc moiety in $[L^1M^{II}]^{2+}$ due to the presence in close proximity of a positively charged metal cation centre. The currents for the new redox couple $[L^1M^{II}]^{2+}/[L^1M^{II}]^{3+}$ (M^{II} = Zn^{II}, Cd^{II}, Hg^{II} and Pb^{II}) increase linearly until one equivalent of the guest metal cation species is added. At this point the reversible oxidation wave corresponding to uncomplexed L^1 disappears (Fig. 5). In the case of Cu^{II}, at the 1 : 1 L^1/Cu^{II} molar ratio, the wave corresponding to the oxidation of the complex species $[L^1Cu^{II}]^{2+}$ disappears with a concomitant rapid change in the solution colour from emerald-green to pale yellow, while only the wave corresponding to free L^1 is left in the cyclic voltammogram. This wave is broader and characterised by lower maximum currents with respect to the electrochemical signal for free L^1 before addition of Cu^{II}. Very likely the initially coordinated Cu^{II} centre is reduced by the Fc moiety of L^1 to Cu^{I}, which is stabilised in this redox state by the interaction with the S-donors of the [12]aneNS$_2$O framework. A similar spontaneous process has been described by Sato *et al* on addition of Cu(BF$_4$)$_2$ to polythia[*n*]ferrocenophanes.[53] However in our case, no oxidation process is observed at higher potentials for a Cu^{I}/Cu^{II} process and the reduction of the Fc$^+$ unit in $[L^1Cu^{I}]^{2+}$ should take place to a potential value very close to that for the couple Fc$^+$/Fc in free L^1.

In contrary to what is observed in the presence of Cu^{II}, Zn^{II}, Cd^{II}, Hg^{II}, or Pb^{II}, a one-wave electrochemical behaviour (Fig. 5d) is observed upon addition of $HClO_4$ to L^1 with an anodic shift of the Fc/Fc$^+$ redox couple by *ca.* 120 mV.

Table 5 Electrochemical cation-dependence of L^1 and L^2 [a]

Receptor	Cation (0.5 equiv. added)	$E_{1/2}^{complex}$/mV	ΔE/mV [b] ($E_{1/2}^{complex} - E_{1/2}^{free\ ionophore}$)	RCE ($K_{neutral}/K_{ox}$) [c]
L^1	H^+	610	120 [d]	
	Cu^{II}	690	200	2432
	Zn^{II}	710	220	5304
	Cd^{II}	620	130	159
	Hg^{II}	570	80	23
	Pb^{II}	700	210	3592
L^2	H^+	630	170 [d]	
	Cu^{II}	690	230	7832
	Zn^{II}	660	200	2432
	Cd^{II}	550	90	33
	Hg^{II}	600	140	235
	Pb^{II}	660	200	2432

[a] Data obtained in MeCN solution containing 0.1 mol dm^{-3} nBu_4NBF_4 as supporting electrolyte, *vs.* Ag/AgCl with a platinum working electrode; solutions were *ca.* 10^{-3} mol dm^{-3} in free receptor (see Experimental). [b] Shift in oxidation potential produced by presence of metal cation (0.5 equivalents); $E_{1/2}^{free\ ionophore}$ = 490 and 460 mV for L^1 and L^2 respectively [$E_{1/2} = (E_{pa} + E_{pc})/2$]. [c] Reaction Coupling Efficiency (RCE), which can be calculated only in the two-wave case (see text).[2,4,6] [d] The behaviour of the redox-responsive ionophores L^1 and L^2 has also been investigated in the presence of $HClO_4$; the redox potential of the ferrocene unit is anodically shifted upon successive additions of H^+ according to a one-wave behaviour. The reported $E_{1/2}$ values refer to the addition of 1 equivalent of H^+.

A two-wave electrochemical behaviour has already been observed by Gokel and co-workers[12] on studying the host–guest interaction between some ferrocene cryptand molecules and alkali metal cations by cyclic voltammetry. The presence of two distinguishable waves in the cyclic voltammogram has been accounted for in terms of the high stability constant for the neutral unoxidised redox-responsive ionophore/metal cation complex and the large difference between the half-wave potentials for the two observed redox couples, with the magnitude of the anodic shift being dependent upon the guest's polarising power.[12] By coupling the electrode oxidation and cation complexation for the neutral ionophore with the electrode oxidation of its metal complex, and the cation complexation for its oxidised form in a one-square scheme, the following equation can be derived[2,4,6,12] according to thermodynamic considerations: $E_{1/2}^{complex} - E_{1/2}^{free\ ionophore} = (RT/nF)\ln(K_{neutral}/K_{ox})$, where $K_{neutral}$ is the metal binding constant for neutral unoxidised redox-responsive ionophore and K_{ox} is the metal binding constant for its oxidised form. The quantity $K_{neutral}/K_{ox}$ has been defined by Beer and co-workers[6] as Reaction Coupling Efficiency (RCE) and together with the shift in oxidation potential produced by presence of metal cation ($E_{1/2}^{complex} - E_{1/2}^{free\ ionophore}$) represents a quantitative measure of the perturbation of the redox centre induced by the guest complexation to the receptor unit; these two quantities can be very useful to evaluate the ability of the redox-responsive ionophore to selectively respond to the host binding of the guest species. The results obtained for L^1 are reported in Table 5. The largest redox shift is observed in the presence of the Zn^{II} and Pb^{II} metal ions with values for ΔE of 220 and 210 mV respectively (Fig. 5a–b). The calculated RCE is 5304 and 3592 for Zn^{II} and Pb^{II} respectively, which means that in the MeCN solution L^1 binds Zn^{II} *ca.* 5×10^3 times more strongly than its oxidised form $[L^1]^+$. Lower redox shifts are observed for Cu^{II} and Hg^{II} (ΔE = 200 and 80 mV, respectively). In the presence of Cd^{II}, the measured electrochemical shift (ΔE = 130) is very close to that observed for L^1 in the presence of $HClO_4$, suggesting that the protonation of the tertiary nitrogen atom of L^1 is taking place rather than the coordination of the metal centre to the macrocyclic framework.[6,54] However, a different electrochemical behaviour is observed for L^1 in the presence of Cd^{II} (two-wave, Fig. 5c) and H^+ (one-wave, Fig. 5d); therefore, the interaction process of Cd^{II} with the [12]aneNS$_2$O unit of L^1 cannot be totally ruled out as also demonstrated by the isolation of the complex $[Cd([12]aneNS_2O)(NO_3)_2]$ (**5**) from the reaction of L^1 with $Cd(NO_3)_2 \cdot 4H_2O$ in MeCN (see above). The electrochemical response of L^1 to the presence of Cu^{II}, Zn^{II}, Cd^{II}, Hg^{II}, or Pb^{II} seems to contrast with the solution studies reported above, which show that Hg^{II} in water has the highest affinity for [12]aneNS$_2$O followed by Cu^{II}, Cd^{II}, Pb^{II}, and Zn^{II}. Presumably, the highest polarising power of Zn^{II} and the different solvation ability of MeCN compared to water, are crucial in determining the through-space-mediated electrostatic interaction with the ferrocene redox centre.

On passing from L^1 to L^2, *i.e.* on replacing the O-donor with an S-donor in the macrocyclic receptor unit, a dramatic change is observed in the redox behaviour of the ferrocene unit in the presence of metal cation guests (see Table 5). In fact, this time, the largest potential shift (ΔE = 230 mV) is recorded for Cu^{II} and not for Zn^{II} (ΔE = 200 mV) in agreement with the N>S>O donor affinity trend generally observed for the former. A shift of 200 mV is also observed in the case of Pb^{II}, whereas a much lower potential shift is observed in the case of Hg^{II} and Cd^{II}, ΔE being 140 and 90 mV, respectively. Interestingly, the response of L^1 and L^2, in terms of ΔE, to the interaction with Cu^{II}, Zn^{II}, Cd^{II}, Hg^{II}, or Pb^{II} reflects the donor affinity trend normally observed for these metal ions with mixed-donor macrocyclic ligands: N>S>O for Cu^{II} and Hg^{II} and N>O>S for Zn^{II}, Cd^{II}, and Pb^{II}. In fact, a decrease in ΔE is observed in the presence of Zn^{II}, Pb^{II}, and Cd^{II} on passing from L^1 to L^2, whereas an increase is recorded for Cu^{II} and Hg^{II} (see Table 5).

On the whole, despite the presence of S-donors in the binding sites of both L^1 and L^2, these two ionophores do not show a selective sensing response to soft metal ions such as Hg^{II} and Cd^{II}, but rather seem to be suitable to detect harder metal ions such as Zn^{II} and Cu^{II} in non-aqueous environment. Interestingly, the analogous ionophore *N*-ferrocenylmethyl 1-aza-4,7,10-trioxacyclododecane (*N*-Fc-[12]aneNO$_3$) which has an NO_3 donor set in the 12-membered macrocyclic receptor unit, exhibits a selective electrochemical response to the heavy metal ions Hg^{II} and Pb^{II}.[54]

Acknowledgements

We thank *Regione Autonoma della Sardegna* and *Università degli Studi di Cagliari* for financial support.

References

1 P. D. Beer, *Chem. Soc. Rev.*, 1989, **18**, 409.
2 P. D. Beer, P. A. Gale and G. Z. Chen, *Coord. Chem. Rev.*, 1999, **185–186**, 3.
3 P. L. Boulas, M. Gómez-Kaifer and L. Echegoyen, *Angew. Chem., Int. Ed.*, 1998, **37**, 216.
4 P. D. Beer and D. K. Smith, *Prog. Inorg. Chem.*, 1997, **46**, 1.

5 R. Martínez-Máñez, J. Soto, J. M. Lloris and T. Pardo, *Trends Inorg. Chem.*, 1998, **5**, 183.
6 P. D. Beer, P. A. Gale and G. Z. Chen, *J. Chem. Soc., Dalton Trans.*, 1999, 1897.
7 A. Ion, J. C. Moutet, E. Saint-Aman, G. Royal, S. Tingry, J. Pecaut, S. Menage and R. Ziessel, *Inorg. Chem.*, 2001, **40**, 3632.
8 J. E. Kingston, L. Ashford, P. D. Beer and M. G. B. Drew, *J. Chem. Soc., Dalton Trans.*, 1999, 251.
9 P. D. Beer, *Chem. Commun.*, 1996, 689.
10 G. C. Dol, P. C. J. Kamer, F. Hartl, P. W. N. M. van Leeuwen and R. J. M. Nolte, *J. Chem. Soc., Dalton Trans.*, 1998, 2083.
11 H. Plenio and R. Diodone, *Inorg. Chem.*, 1995, **34**, 3964.
12 J. C. Medina, T. T. Goodnow, M. T. Rojas, J. L. Atwood, B. C. Lynn, A. E. Kaifer and G. W. Gokel, *J. Am. Chem. Soc.*, 1992, **114**, 10583.
13 M. C. Grossel, D. G. Hamilton, J. I. Fuller and E. Millan-Barios, *J. Chem. Soc., Dalton Trans.*, 1997, 3471.
14 M. C. Grossel, M. R. Goldspink, J. A. Hriljac and S. C. Weston, *Organometallics*, 1991, **10**, 851.
15 J. M. Lloris, R. Martínez-Máñez, M. E. Padilla-Tosta, T. Pardo, J. Soto, P. D. Beer, J. Cadman and D. K. Smith, *J. Chem. Soc., Dalton Trans.*, 1999, 2359.
16 P. D. Beer, Z. Chen and M. I. Ogden, *J. Chem. Soc., Faraday Trans.*, 1995, **91**, 295.
17 P. D. Beer, Z. Chen, M. G. B. Drew and A. J. Pilgrim, *Inorg. Chim. Acta*, 1994, **225**, 137.
18 P. D. Beer and P. V. Bernhardt, *J. Chem. Soc., Dalton Trans.*, 2001, 1428.
19 J. M. Lloris, R. Martínez-Máñez, T. Pardo, J. Soto and M. E. Padilla-Tosta, *J. Chem. Soc., Dalton Trans.*, 1998, 2635.
20 P. D. Beer, J. Cadman, J. M. Lloris, R. Martínez-Máñez, J. Soto, T. Pardo and D. Marcos, *J. Chem. Soc., Dalton Trans.*, 2000, 1805.
21 P. D. Beer, J. E. Nation, S. L. W. McWhinnie, M. E. Harman, M. B. Hursthouse, M. I. Ogden and A. H. White, *J. Chem. Soc., Dalton Trans.*, 1991, 2485.
22 L. G. A. van de Water, F. ten Hoonte, W. L. Driessen, J. Reedijk and D. C. Sherrington, *Inorg. Chim. Acta*, 2000, **303**, 77.
23 L. G. A. van de Water, W. Bujis, W. L. Driessen and J. Reedijk, *New J. Chem.*, 2001, **25**, 243.
24 D. Lednicer and C. R. Hauser, *Org. Synth.*, 1960, **40**, 31.
25 C. Bazzicalupi, A. Bencini, V. Fusi, C. Giorgi, P. Paoletti and B. Valtancoli, *Inorg. Chem.*, 1998, **37**, 941.
26 G. Gran, *Analyst*, London, 1952, 77, 661.
27 P. Gans, A. Sabatini and A. Vacca, *Talanta*, 1996, **43**, 807.
28 SADABS Area-Detector Absorption Correction Program, Bruker AXS, Inc., Madison, WI, USA, 2000.
29 G. M. Sheldrick, SHELXS 86-97, *Acta Crystallogr., Sect. A*, 1990, **46**, 467.
30 G. M. Sheldrick, SHELXL 93-97, Universität Göttingen, Germany, 1997.
31 P. V. Bernhardt and G. A. Lawrance, *Coord. Chem. Rev.*, 1990, **104**, 297.
32 A. J. Blake and M. Schröder, *Adv. Inorg. Chem.*, 1990, **35**, 1.
33 A. Bencini, A. Bianchi, E. Garcia-España, M. Micheloni and J. A. Ramirez, *Coord. Chem. Rev.*, 1999, **188**, 97.
34 V. J. Thöm, M. S. Shaikjee and R. D. Hancock, *Inorg. Chem.*, 1986, **25**, 2992.
35 M. T. S. Amorin, S. Chaves, R. Delgado and J. J. R. Fraústo da Silva, *J. Chem. Soc., Dalton Trans.*, 1991, 3065.
36 S. T. Marcus, P. V. Bernhardt, L. Grøndahl and L. R. Gahan, *Polyhedron*, 1999, **18**, 3451.
37 K. A. Byriel, L. R. Gahan, C. H. L. Kennard and C. J. Sunderland, *J. Chem. Soc., Dalton Trans.*, 1993, 625.
38 R. M. Izatt, K. Pawlak, J. S. Bradshaw and R. L. Bruening, *Chem. Rev.*, 1991, **91**, 1721.
39 S. Afshar, S. T. Marcus, L. R. Gahan and T. W. Hambley, *Aust. J. Chem.*, 1999, **52**, 1.
40 D. St. C. Black and I. A. McLean, *Aust. J. Chem.*, 1971, **24**, 1401.
41 M. T. Youinou, J. A. Osborn, J.-P. Collin and P. Lagrange, *Inorg. Chem.*, 1986, **25**, 453.
42 M. Micheloni, P. Paoletti, L. Siegfried-Hertli and T. A. Kaden, *J. Chem. Soc., Dalton Trans.*, 1985, 1169.
43 T. A. Kaden, S. Kaderli, W. Sager, L. C. Siegfried-Hertli and A. D. ZuberBuhler, *Helv. Chim. Acta*, 1986, **69**, 1216.
44 M. Kodama, T. Koike, N. Hoshiga, R. Machida and E. Kimura, *J. Chem. Soc., Dalton Trans.*, 1984, 673.
45 M. Kodama and E. Kimura, *J. Chem. Soc., Dalton Trans.*, 1976, 116.
46 M. Kodama and E. Kimura, *J. Chem. Soc., Dalton Trans.*, 1977, 2269.
47 M. Kodama and E. Kimura, *J. Chem. Soc., Dalton Trans.*, 1976, 2335.
48 V. J. Thom, G. D. Hosken and R. D. Hancock, *Inorg. Chem.*, 1985, **24**, 3378.
49 F. Arnau-Neu, M. Sanchez, M.-J. Schwing-Weill and J.-M. Lehn, *Helv. Chim. Acta*, 1985, **68**, 456.
50 K. A. Byriel, K. R. Dunster, L. R. Gahn, C. H. L. Kennard, J. L. Latten and I. L. Swann, *Inorg. Chim. Acta*, 1993, **205**, 191.
51 R. D. Hancock, M. S. Shaikjee, S. M. Dobson and J. C. A. Boeyens, *Inorg. Chim. Acta*, 1988, **154**, 229.
52 A. Bondi, *J. Phys. Chem.*, 1964, **68**, 441.
53 M. Sato, M. Katada, S. Nakashima, H. Sano and S. Akabori, *J. Chem. Soc., Dalton Trans.*, 1990, 1979.
54 J. M. Lloris, R. Martínez-Máñez and J. Soto, *J. Organomet. Chem.*, 2001, **637–639**, 151.